Effect of Maleic Anhydride Grafted Ethylene Vinyl Acetate Compatibilizer on the Mechanical, Thermal Properties and Weathering Resistance of Polyamide 11/Bamboo Fiber Composite

Mai Duc Huynh[1], Tran Huu Trung[1], Do Van Cong[1], Thai Hoang[1], Eric Dantras[2], Colette Lacabanne[2] and Nguyen Vu Giang[1,*]

[1]*Department of Physico-Chemistry of Non-Metallic Material, Institute for Tropical Technology, Vietnam Academy of Science and Technology, Hanoi, Vietnam*
[2]*Institut Carnot CIRIMAT, Université Paul Sabatier, 31 062 Toulouse Cedex 09, France*

In this research, short bamboo fiber (BF) has been used as filler in the fabrication of the composite based on polyamide 11 (PA11) by melt-mixing method. In order to improve the compatibility between BF and PA11, maleic anhydride grafted ethylene vinyl acetate copolymer (EVAgMA) was introduced into the composite preparation process. The effect of EVAgMA contents on mechanical, thermal or weathering resistant properties of the composites was investigated. In the presence of the EVAgMA, the tensile strength, impact strength and flexural modulus of composites showed the improvement in comparison to without compatibilizer. Differential scanning calorimetry (DSC) analysis indicated that the melting temperature of composites did not depend on the EVAgMA contents, while its fusion heat (ΔHm) decreased with increasing EVAgMA contents. Dynamic mechanical thermal analysis (DMTA) evaluated the role of EVAgMA on the enhancement of composites's storage modulus (G′) in the glassy plateau and the interaction between BF and PA11 matrix. After 840 hours of accelerated weathering test, the composites using EVAgMA were decomposed faster than that of neat PA11 and PA11/BF composite. This result was also agreed with the observation of scanning electronic microscopy (SEM) images and the change of carbonyl index (CI). However, the retention of tensile properties of PA11/EVAgMA/BF composites is higher than that of PA11/BF composite. [doi:10.2320/matertrans.MT-MN2019001]

Keywords: *polymer composite, short bamboo fiber, EVAgMA compatibilizer, weathering resistance, mechanical properties*

1. Introduction

Recently, the natural fiber composites (NFC) have been received more and more attention thanks to their potential as the replacement for reinforced synthetic fiber of composites. In which, natural fibers such as: jute, hemp, kenaf, bamboo play as important components in composites, affecting strongly mechanical performance of NFC.[1)] Among them, short bamboo fiber (BF) has many outstanding advantages with low density, high specific strength, stiffness.[2)] Besides, bamboo can be found in almost all continents (except Europe) with the fastest growth rate among plants. Hence, BF is considered as a cheap raw material and could meet a large required amount in the many sectors, including polymer composites. However, the weak thermal stability of BF is one of the main challenges to broaden its further application. Like other natural fibers, degradation of BF occurs at about 200°C.[3,4)] BF is mainly used as the reinforcement filler to soften resins which have low temperature processing (below 200°C) such as polypropylene (PP), polyethylene (PE) or polyvinyl chloride (PVC).[5)] These polymers are synthesized from fossil sources such as coal, petroleum that can cause environmental impacts such as carbon dioxide emissions, restoration ecology. Therefore, the bio-polymers or polymers derived from biomass are considered as potential alternatives to conventional polymers. Some researchers investigated the effect of BF on the mechanical properties of biocomposites using biopolymers such as: polybutylenesuccinate (PBS),[6)] polylactic acid (PLA).[7,8)] In this regard, polyamide 11 (PA11) is known as one of the most popular biopolymers with outstanding mechanical properties and melting temperature at about 190°C.[9)] The combination between PA11 resin and BF is expected to create the biocomposite with high mechanical properties and environmentally friendly. However, the literatures related to BF-reinforced PA11 composites are not mentioned much.[10)] The natural fibers that were used as reinforcement for PA11 resin are short wood fiber like pine and beech….[11–13)] As a nature, the interaction between BF and PA11 matrix is quite poor that could affect on mechanical performance of PA11 based composite. Therefore, the improvement of interfacial adhesion between BF and PA11 resin is the key to fabricate PA11/BF composites with high mechanical properties. Patrick Zierdt[11)] treated beech fiber with sodium hydroxide (NaOH concentration 10 g/l) to improve compatibility with PA11. Accordingly, for bio-composite with 50 wt% beech fiber, E-modulus increased about 8% by chemical treatment of the fiber while tensile strength significantly unchanged. Helena Oliver-Ortega *et al.*[12)] treated stone ground wood fibers in an oven at 165°C for 1 hour. After annealing, the crystallinity of PA11 composites with high fiber contents increased and led to the higher impact on mechanical behavior. Another method to improve the compatibility of NFC is to introduce specific functional groups into polymers which could interact with components in composites. The copolymers such as maleated polypropylene (MAPP) or maleated polyethylene (MAPE) have been reported in many researches to be such effective compatibilizers.[14–17)] Maleic anhydride groups grafted to copolymer could covalently link with hydroxyl groups in cellulosic fiber to form an ester linkage, leading to an improvement in interfacial adhesion between the polymeric matrix and the fiber.[16,17)] Consequently, tensile strength, bending modulus and impact strength of composites could be significantly enhanced. Some studies found that maleic

*Corresponding author, E-mail: nvgiang@itt.vast.vn

Table 1 The component of PA11/BF composites with different EVAgMA contents.

Sample code	PA11 content (wt.%)	BF content (wt.%)	EVAgMA content (wt.%)
PA11	100	0	0
PA030	70	30	0
PA230	68	30	2
PA430	66	30	4

anhydride groups of polymers can interact with the amino end groups of polyamide at the interface.[18,19] However, the works using anhydride maleic grafted polymers as compatibilizer for PA11/natural fiber composite have not been mentioned much. Maleic anhydride grafted ethylene vinyl-acetate copolymer (EVAgMA) is expected to improve the dispersibility of BF into PA11 matrix and enhance the mechanical properties of PA11/natural fiber composites. Moreover, due to low viscosity of EVAgMA, processing of PA11/EVAgMA/BF composites could be more convenient for industrial production.

In previous study, we used the tetraethyl orthosilicate (TEOS) to modify BF as the filler at different contents for PA11.[20] The results showed that modified BF significantly improved the storage module (G′) and the compatibility between phases in composite. However, the modification of BF by silane solution faced some problems while real industrial processing, for example: solvent treatment, solution mixing, drying, environmental pollution. The aim of this study is to replacement the modification of BF by using a compatibilizer such as EVAgMA to enhance the interaction of BF and PA11. This article evaluated the mechanical properties, thermal properties and the weathering resistance of PA11/BF composites. In order to clarify the role of EVAgMA as a compatibilizer, the BF content kept constant at 30 wt% for all composites.

2. Experimental

2.1 Materials

Polyamide 11 (PA11) with the trade name Arkema Rilsan® BESNO P20 was the product of Akerma (France), with density of 1.04 g cm^{-3} and a melting temperature of 184°C. The BF was supplied by Vietnam Wood processing Company Limited (Vietnam) with average fiber diameter smaller than 150 µm. Ethylene vinyl acetate copolymers (EVA) containing 18 wt% of vinyl acetate with density of 0.93 g cm^{-3} were purchased from Honam Petrochemical Corporation (Korea). Maleic anhydride (MA) and dicumyl peroxide (DCP) with purity of 99.0 and 99.8%, respectively, were purchased from Merck (Germany). EVAgMA pellets were prepared in melt mixing state by PolyHaake extruder at Institute for Tropical Technology, VAST. The weight ratio of EVA:DCP:MA was fixed at 100:0.3:3.[21,22]

2.2 PA11/BF composite preparation

The composite was prepared by a Haake Rheomix 610 mixer at 195°C with the rotor speed of 50 rpm. Sample weight including PA11, EVAgMA and BF was calculated to keep filler factor constant at around 0.7 of mixing chamber volume as shown in Table 1. Firstly, the melt compound of PA11 and EVAgMA was performed for 4 minutes before adding BF into the hot chamber and keep mixing for next 4 minutes to reach paste state. Next, the paste material was quickly hot pressed at 210°C into the sheet with thickness of 2 mm by using a hot press machine (Tokyoseiki, Japan) for 3 minutes under pressure of 20 MPa. Finally, the obtained samples were cooled down and stored at room temperature for at least 24 hours before using for further analysis.

2.3 Characterization

2.3.1 Melting rheology characterization

Melting rheology data was collected by using a Haake Polylab System simulating software on Haake Rheomix 610 mixer (Germany).

2.3.2 Tensile strength, young modulus and elongation at break measurements

Tensile strength, Young modulus and elongation at break of the composites were determined at the same time on a Zwick Tensile 2.5 Machine (Germany) according to ASTM D638 standard.

2.3.3 Impact strength measurement

Izod impact strength measurement of samples was conducted on a 402D-Z2 machine (Testresources, USA) at temperature of 22°C and the humidity of 40% according to ASTM D256 standard.

2.3.4 Flexural strength

The flexural strength of samples was tested according to ASTM D790 standard on an Instron equipment (USA) at temperature of 22°C and the humidity of 40%.

2.3.5 Differential scanning calorimetry (DSC)

DSC analysis was performed on a DSC 204F1 equipment (Perkin Elmer, USA). The samples were analysed with the temperature ranged from 20 to 150°C and the heating rate of 20°C min^{-1}.

2.3.6 Weathering test

Weathering test was carried out according to ASTM G154 standard. In which, samples were exposed with 8 hours of UV irradiation at 60°C then 4 hours of humidity condensation at 50°C in UV-CON equipment (USA). This 12 hours weathering cycle was repeated for 70 times until total of 840 hours.

2.3.7 Attenuated total reflection Fourier transform infrared analysis (ATR-FTIR)

The ATR-FTIR analysis was carried out in the range of 4000–400 cm^{-1} with the resolution of 16 cm^{-1} at room temperature by using a Nicolet iS10 equipment (Thermo Sciencetific, USA). Following the approach described by

Stark and Matuana, the peak intensities of absorption bands at 1715 and 2915 cm^{-1} were used to calculate carbonyl index according to the following equation:[23)]

$$\text{Carbonyl index} = \frac{I_{1715}}{I_{2915}} \times 100$$

2.3.8 Dynamic shear modulus

The storage modulus G′ and loss modulus G″ of the samples were obtained from dynamic shear modulus analysis by using a MCR 302 (Anton Paar, Austria) equipment. Samples were prepared as the 50 × 10 × 0.65 mm size. The analysises were carried out under nitrogen atmosphere and temperature range from −120°C to 150°C, heat rate of 3°C min^{-1}, an angular frequency of applied force 1 $rads^{-1}$ and dynamic strain of 0.1%.

2.3.9 Morphogical analysis

Scanning electron microscopy (SEM) was performed by JSM 6510 LV equipment (JEOL, Japan) to observe the change of the surface of samples before and after accelerated weathering test.

3. Results and Discussion

3.1 Melting rheology behavior

The torque diagrams of neat PA11 and PA030, PA230 and PA430 composites were recorded by Polylab software and shown in Fig. 1. Torque diagram of PA11 sample reached the maximum value immediately after closing the mixing chamber. This increase in torque was caused by the friction between PA11 pellets and twin-screw in the mixing chamber. By transferring the heat from hot metal surface of chamber into the resin, PA11 slightly melted and resulting a decrease of torque. Material became almost melting state at the 3rd minute because the torque has not changed significantly in this stage. In case of the composites, the their torque behaviors were similar to PA11 sample in the first half of the mixing process. However, the mixture of PA11 and EVAgMA accounting for 70 wt% of the total weight of samples caused the lower torque in comparison with PA11. At the 4th minute, the second peak appeared after adding 30 wt% of BF, this leaded to a significant increase of torque for composites. Clearly, PA030 sample showed the highest torque while PA230 and PA430 samples showed lower values in range from the 5th minute to the 8th minute. It found that EVAgMA caused a decrease in torque by its lower viscosity. Thus, the usage of EVAgMA might effectively reduce the processing viscosity of low flux melting polymers such as polyamide resin.

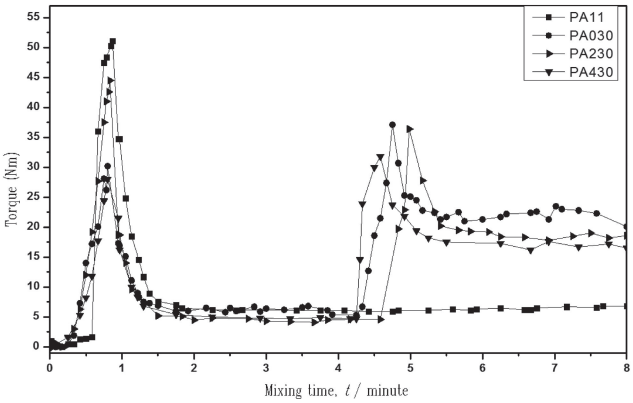

Fig. 1 Torque diagrams of neat PA11, PA030, PA230 and PA430.

3.2 Mechanical properties

Table 2 shows the mechanical properties of the neat PA11, PA030, PA230 and PA430 composites. Tensile strength of PA11 reached 32.0 MPa, which is consistent with published data of the manufacturer. By adding 30 wt% of BF into PA11, tensile strength of the composite increased up to 38.5 MPa. This improvement can be attributed to the hydrogen bonding between PA11 resin and BF. This linkage could promote the dispersion of BF; thus, the stress is uniformly distributed at the interphase, improving tensile strength of composite. According to Patrick Zierdt,[16)] an increase in the fiber content also leads a slight improve in tensile strength of the composite in comparison with PA11. At the loading of 2 wt% of EVAgMA, the tensile strength of composite reached the highest value of 40.1 MPa. Tensile strength of the composites changed not much when content of EVAgMA increased up to 4 wt%. This may be due to an excess EVAgMA amount reduced the stress transfer from PA11 to BF. These results showed that 2 wt% of EVAgMA could promote a fine dispersion of BF in PA11 matrix and improve the tensile strength of PA11/BF composites.

Young's modulus of PA11 was 300.0 MPa, this showed an increase of 2.66 times by adding of 30 wt% BF into PA11. This is common in PA/BF composites due to the partly replacement of PA11 by rigid BF in the composite.[11)] In the presence of EVAgMA, Young modulus of the composites had a tendency of decrease but still higher than that of neat PA11. The utilization of EVAgMA with low elastic modulus could cause the decrease in Young's modulus, which is consistent with the results Chattopadhyay reported,[17)] Young's modulus of polyproplylene/BF composites slightly decrease in addition of MAPP. On the other hand, the presence of BF

Table 2 The mechanical characteristics of original PA11 and PA11/BF composites.

Samples	Tensile strength (MPa)	Elongation at break (%)	Young's modulus (MPa)	Impact strength (kJ/m^2)	Flexural strength (MPa)	Flexural modulus (MPa)
PA11	32.0	252.2	300.0	unbroken	13.1	310.9
PA030	38.5	8.3	797.7	5.3	20.4	562.3
PA230	40.1	12.1	527.9	7.0	25.0	721.7
PA430	39.7	16.3	597.8	6.5	27.5	654.5

in PA11 composites caused a rapid decrease in elongation at break from 252% down to 8.3% for PA030 sample due to the increase in the discontinuity of PA11 matrix. However, PA230 and PA430 showed a slight improvement in elongation at break because of addition of EVAgMA.

Similarly, the flexural moduli of PA11/BF composites highlight the significant improvement. At the loading of 30 wt% BF, flexural modulus remarkably increased to 562.3 MPa in comparison to neat PA11 (310.9 MPa). The improvement of the flexural modulus may be related to the increase of stiffness of the composites. It is found that the flexural modulus of PA230 sample was strongly increased by 28.3% up to 721.7 MPa in comparison with the PA030 sample. Whereas, for the case of PA430 composite containing 4 wt% of EVAgMA, flexural modulus was measured at 654.5 MPa, corresponding to a slight increase (about 9.3%) compared to that of PA030 sample. The excess EVAgMA in PA430 might lead to the separation of phases in the composites. Moreover, the presence of EVAgMA also increased considerably flexural strength from 20.4 MPa to 25.0 MPa for the case of PA230 sample. Interestingly, as the compatibilizer content increased up 4 wt%, flexural strength showed an improvement, about 9.2% higher than that of the PA230 sample.

Concerning to the impact strength, neat PA11 matrix was unbroken due to its high elastic. For the case of PA030 sample, the impact strength was recorded at 5.3 kJ m^{-2}. The addition of EVAgMA into PA230 and PA430 provided a significant increase in the impact strength of composites, about 7.0 and 6.5 kJ m^{-2}, respectively. This improvement could be expected that EVAgMA can interact with both hydroxyl groups of BF and the amino end groups of PA11, resulting in the formation of a good interfacial adhesion. Therefore, stress could transfer efficiently along the bulk composite.

3.3 Differential scanning calorimetry analysis (DSC)

Figure 2 presents the DSC diagrams of PA11, PA030, PA230 and PA430 samples. The melting temperature of PA11 was recorded at 184.6°C.[24,25] In the presence of BF and EVAgMA, the melting temperature of the composites was not significantly affected (Table 3).[24] However, the fusion heat (ΔHm) of the composite which is the energy for phase transition from solid state to melting state was decreased by the presence of BF and EVAgMA in comparison to original PA11. Specifically, ΔHm of PA430 sample dropped down to 18.70 J g^{-1} compared with 32.18 J g^{-1} of original PA11 sample for. S.H. Lee explained that the decrease may be also attributed to the strong interfacial interaction between polymer matrix and BF.[6]

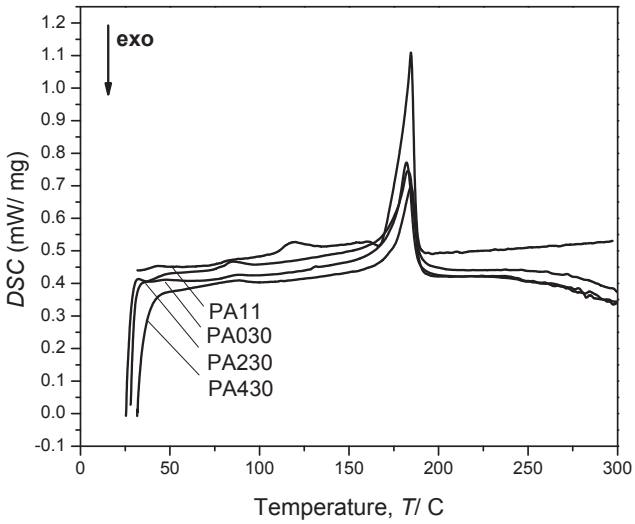

Fig. 2 DSC diagrams of PA11, PA030, PA230 and PA430 composites.

3.4 Dynamic shear modulus

Figure 3 shows the dynamic mechanical behavior of PA11, PA030, PA230 and P430 composites in the temperature range from −120°C to 100°C. Dynamic storage modulus behavior (G′) undergoes the glassy plateau (below Tg) and rubbery plateau (from Tg to Tm) regions.

In the glassy plateau, by addition of BF, G′ of the composites improved in comparison to that of PA11 (Fig. 3(a)). The improvement of these moduli can be explained by hydrogen bonds between hydroxyl groups of BF and amide groups of PA11.[11] The PA230 shows a dynamic modulus improvement in the glassy plateau, thanks to compatibility of EVAgMA with PA11 and BF. However, with addition of 4 wt% of EVAgMA, the G′ values are reduced (PA430 sample). This may be due to the higher EVAgMA content reduced the stress transfer efficiency from the PA11 resin to the reinforcing fillers.

In the rubbery plateau, the storage module of composite reached the same value, it means that EVAgMA has no influence on the rubbery phase. This is similar to our previous studies, when using modified BF with tetraethyl orthosilicate (TEOS), it had no change on shear storage modulus in the rubbery plateau.[20,26]

Figure 3(b) presents the loss modulus of PA11 and PA11/BF composites with different EVAgMA contents. It can be seen that two β and α relaxations at about −80°C and −7°C, respectively. The β relaxation is related to the free amide group, while another peak is associated with the glass transition. β relaxation of the composites was observed at higher temperature than that of PA11, which indicated the

Table 3 Melting behaviour of PA11 and PA11/BF composites with various EVAgMA contents.

Sample	Melting temperature (°C)	ΔHm (J/g)
PA11	184.6	32.18
PA030	182.1	31.35
PA230	182.8	23.94
PA430	184.7	18.70

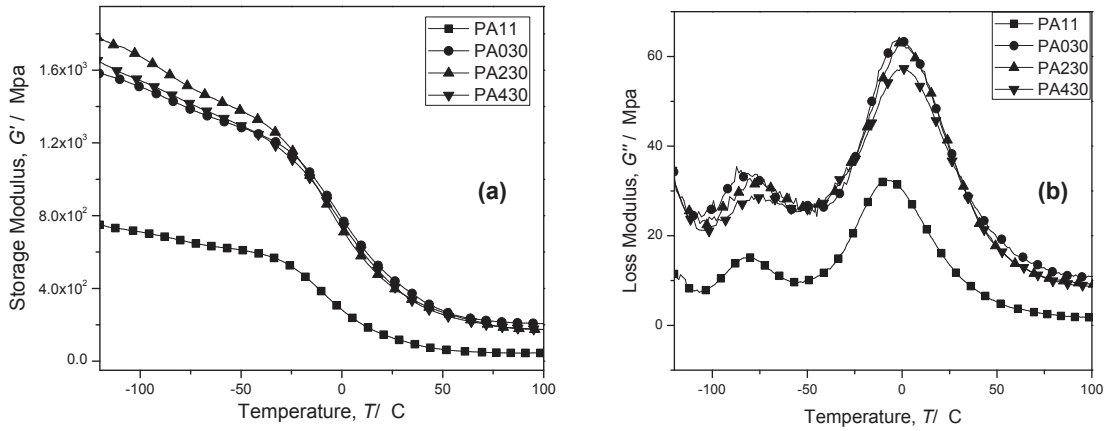

Fig. 3 Storage modulus G′ (a) and loss modulus G″ (b) versus temperature for PA11 and the PA11/BF composite.

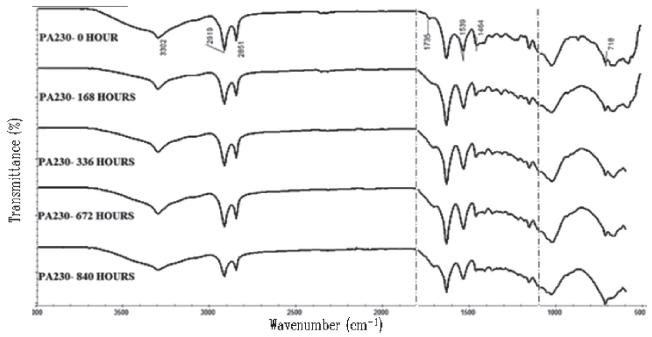

Fig. 4 ATR-FTIR spectra of PA230 sample at different testing time: 0, 168, 336, 672 and 840 hours.

physical interaction at interphase of PA11/BF caused the reduction in the mobility of PA11. The α relaxation is associated with the an elastic mobility liberated at the glass transition. For the case of PA11/BF composites, the typical relaxation consists of two components: the lower-temperature one due to neat polyamide and a higher-temperature one associated with PA11/BF amorphous domains with a lower thermal conductivity.[20)]

3.5 Weathering resistance ability

3.5.1 ATR-FTIR spectra

ATR-FTIR spectra of PA230 sample with different testing time are shown in Fig. 4. All ATR-FTIR spectra showed typical vibration of both PA11 and BF. In detail, the vibration at 3302; 2918 and 2850 cm^{-1} related to amine and methylene (CH_2) groups of PA11, respectively. The bands at 1636 cm^{-1} and 1539 cm^{-1} are considered as the vibration of the 1-level and the 2-level amine groups.[27)] In addition, the typical peaks of BF are also seen at 1711–1739 cm^{-1} regarding the C=O groups in the ester and peak at 1032 cm^{-1} characterizing for C–O linkage of cellulose. After being 840 hours tested, some FTIR peaks of composites had some changes in the intensity and width, especially the peaks at 3302, 1636, 1539 and 1032 cm^{-1}. These changes were attributed to the decomposition of PA11 chains increased the number of carbonyl groups. It is worth noting that the strong shift of the C=O group in ester form from 1735 cm^{-1} to 1709 cm^{-1} (Fig. 5). It is related to the vibration of C=O group in acid form which was formed by degradation of PA11 and lignin in BF. B. Marek also reported that degradation of polyamide is generally considered to proceed by a free-radical mechanism which leads to the formation of peroxides including amines, amides, mono- and di-carboxylic acids, carbon dioxide.[28)]

Analysis of the carbonyl index (CI) obtained from IR spectrum could clarify the decomposition of composites. CI of composite samples has changed significantly against testing time (Table 4). For neat PA11, CI increased steadily over time and reached twofold after 672 hours testing. However, as the testing time increased up to 840 hours, CI slightly decreased. It may be due to a washout (occur in condensation cycle of the test) of short polar substances (which were resulted during the degradation of polymers) on the sample surface. The PA030 composite has also showed a similar trend, but its CI reached the maximum value at 336 hours, reached 2.3 times higher than the value of the initial PA030 sample. This means that the PA030 sample decomposed stronger than the PA11 sample did. Comparing to PA030 sample, PA230 and PA430 samples revealed the faster decomposition and depended on the EVAgMA content. PA430 sample had highest CI, up to 3.6 times higher than that of initial PA430. Obviously, EVAgMA played a role as an initiator for UV decomposition reaction which promoted the degradation of composite.

3.5.2 SEM images of PA11 and PA11/BF composites before and after testing

The surface morphological change of neat PA11 and its composites before and after 840 hours weather accelerated test are clearly seen in Fig. 6. Before testing, the surface of PA11 and composite samples are relatively smooth (Fig. 6(a) and 6(b)). However, there are a few small cracks found on the surface that can be defects during processing. This is a typical surface of PA/BF composites before testing.

After 840 hours weather test, the surface of samples is damaged. For PA11 sample, there are a few discontinuous cracks on the surface because of high UV resistance of PA11. On the contrary, the surface of PA030 samples appeared many cracks; these seem an expansion of initial defects, which speed up the penetration of water as well as degradation agents into the material, promoted the decomposition and reduced mechanical properties. Whereas, for the composites with EVAgMA, the surface destruction is clearly seen, especially for the case of PA430 sample. There are

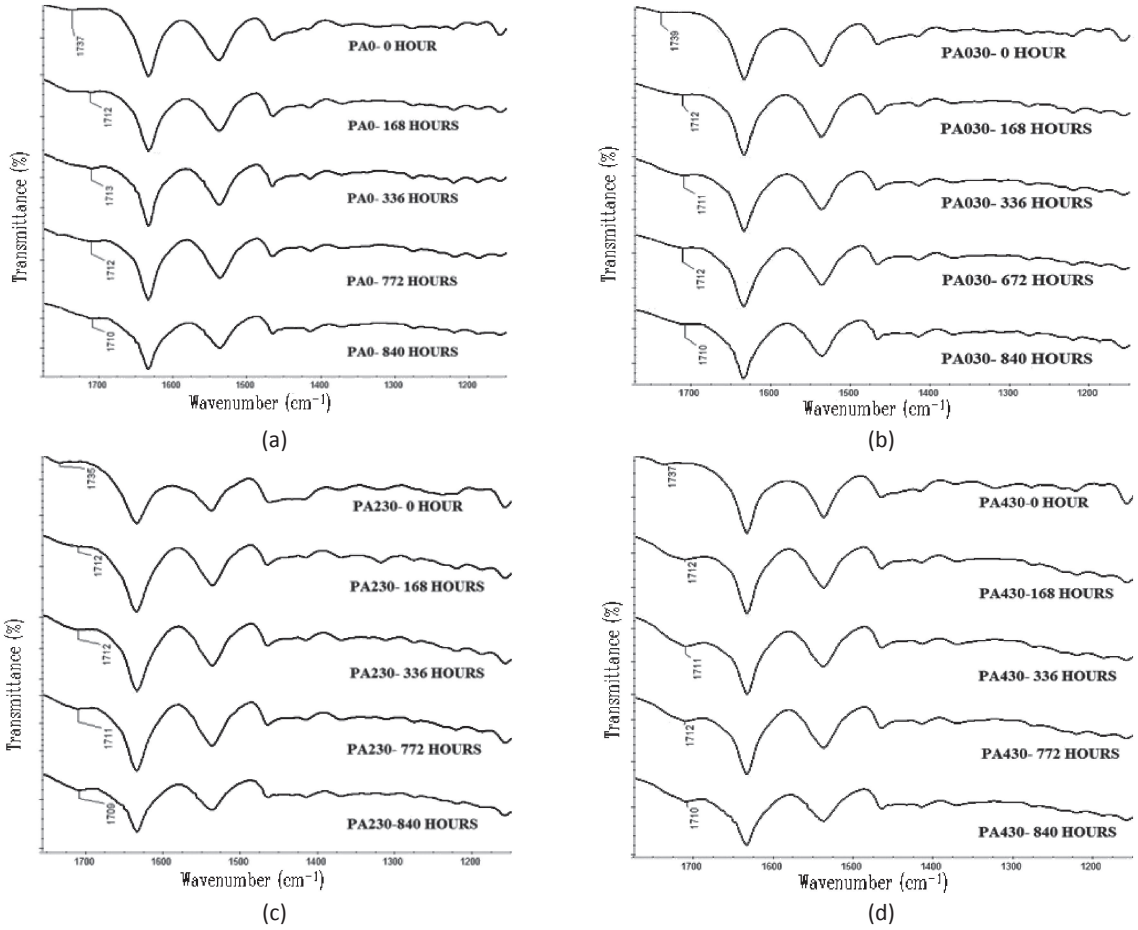

Fig. 5 Vibrations of carbonyl of (a) PA11, (b) PA030, (c) PA230 and (d) PA430 at different testing time.

Table 4 The carbonyl index (CI) of PA11 and PA11/BF composites during weathering test.

Sample / Testing time	PA0	PA030	PA230	PA430
0 hour	6.2	5.8	7.4	8.4
168 hours	7.3	9.4	11.7	25.3
336 hours	11.4	13.7	18.1	30.5
672 hours	12.0	10.9	15.0	24.9
840 hours	11.8	11.5	15.4	16.4

wider and deeper cracks those exposure BF on the surface of samples. Under the influence of UV radiations, EVAgMA was easily decomposed into free radicals that could attack PA11 and BF to promote the photo-degradation. It confirmed that both PA230 and PA430 samples showed stronger oxidation than that of PA030.

3.5.3 Tensile strength retention of PA11 and PA11/BF composites after accelerated weathering test

To evaluate the effect of BF and EVAgMA contents on the weathering resistance, the percent retention (%) of tensile strength and Young's modulus of PA11 and PA11/BF composites were determined after 336 hours and 840 hours.

It can be seen from Fig. 7, PA11 sample has the highest retention of tensile strength and Young's modulus corresponding to 90% and 95%, respectively. Whereas, PA030 sample showed a strong decrease in tensile strength and Young's modulus with introducing 30 wt% BF. It indicated that the change in mechanical properties can be attributed to degradation of BF under UV light. Furthermore, the poor compatibility between PA11 and BF can form voids leading to penetration of water. It caused the destruction in whole bulk of PA030. It is worth noting that the percent of retention (%) of PA230 and PA430 showed a slight improvement with increasing EVAgMA content. This is in contrast to the observation of SEM images, surface of PA230 and PA430 were strongly destroyed by presence of EVAgMA. However, this phenomenon may be only occured on the surface without affecting on internal structure. In the other hand, EVAgMA might improve the compatibility at interphase of composites and form a tight structure that prevented the penetration of

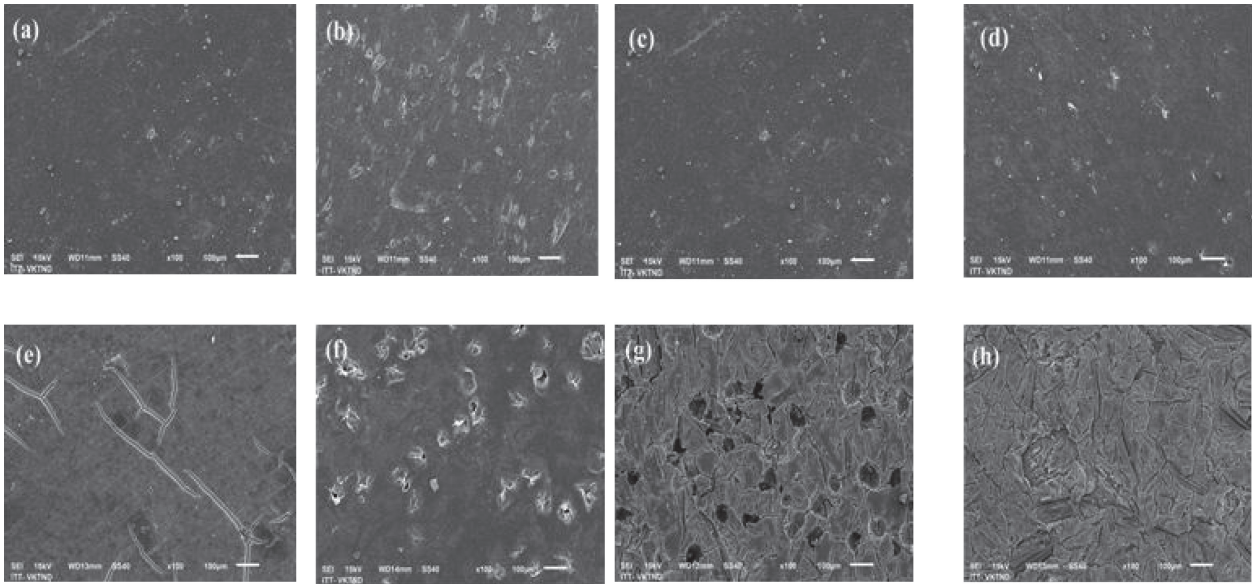

Fig. 6 SEM images of surface samples: (a) PA11, (b) PA030, (c) PA230 and (d) PA430 before testing; (e) PA0, (f) PA030, (g) PA230 and (h) PA430 after testing for 840 hours.

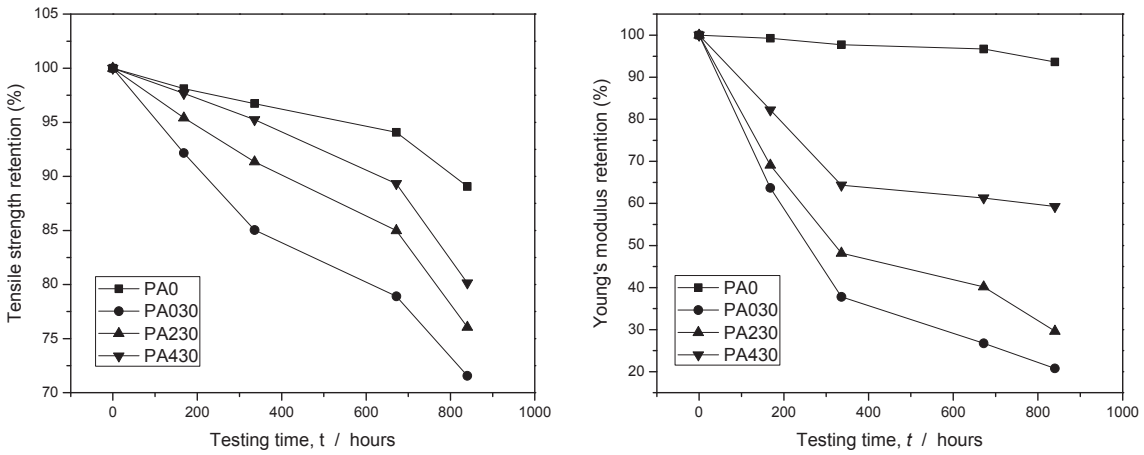

Fig. 7 Tensile properties retention of PA11 and PA11/BF composites after accelerated weathering test.

the water into structure of composite, therefore limite the degradation of properties in comparison to the PA030.

4. Conclusions

The PA11/BF composites were successfully prepared by melt mixing method, the mechanical properties of the composites were improved with the addition of EVAgMA compatibilizer. By adding 2 wt% of EVAgMA, tensile strength, impact strength and flexural strength of the composites containing 30 wt% BF increased by 5, 32 and 25% in comparison to pristine composite, respectively. The differences of ΔHm determined by DSC analysis and G′ and G″ obtained by DMTA of samples proved that EVAgMA could enhance the interaction of BF filler and PA11 matrix. After 840 hours of weathering test, PA/BF composites were decomposed faster than neat PA as observation on SEM images. Naturally, the mechanical properties of composites decreased versus weathering test time because of the penetration of oxidation agents into the interface between phases and the carbonyl index grew up with the increase of EVAgMA content in the composite.

Acknowledgment

This research is financial supported by Vietnam Academy of Science and Technology (VAST) under grant number QTFR01.03/18-19.

REFERENCES

1) K.L. Pickering, M.G.A. Efendy and T.M. Le: Compos., Part A **83** (2016) 98–112.
2) S. Sreenivasulu and A. Chennakeshava Reddy: Int. J. Eng. Res. **3**(1) (2014) 187–194.
3) N.A.R. Sena, M.A.M. Araujo, F.V.D. Souza, L.H.C. Mattoso and J.M. Marconcini: Ind. Crops Prod. **43** (2013) 529–537.
4) J.R. Araújo, W.R. Waldman and M.A. De Paoli: Polym. Degrad. Stabil. **93** (2008) 1770–1775.
5) S. Dos, P.A. Giriolli, J.C. Amarasekera and J.G. Moraes: 8th Annual Automotive Composites Conference and Exhibition (ACCE 2008), (SPE Automotive & Composites Division, Troy, MI, 2008) pp. 492–

500.
6) S.H. Lee and S. Wang: Compos., Part A **37** (2006) 80–91.
7) T. Mukherjee and N. Kao: J. Polym. Environ. **19** (2011) 714–725.
8) R. Sukmawan, H. Takagi and A.N. Nakagaito: Compos., Part B **84** (2016) 9–16.
9) M. Winnacker and R. Bernhard: Macromol. Rapid Commun. **37** (2016) 1391–1413.
10) H. Oliver-Ortega, J.A. Méndez, R. Reixach, F.X. Espinach, M. Ardanuy and P. Mutjé: Polymers (Basel) **10** (2018) 440.
11) P. Zierdt and A. Weber: Mater. Sci. Forum **825–826** (2015) 1039–1046.
12) H. Oliver-Ortega, J.A. Méndez, P. Mutjé, Q. Tarrés, F.X. Espinach and M. Ardanuy: Polymers (Basel) **9** (2017) 522.
13) P. Zierdt, G. Kulkarni and T. Theumer: Macromol. Symp. **373** (2017) 1600118.
14) M. Ossi and K. Timo: Recycling **4**, 6 (2019).
15) A.L. Catto, L.S. Montagna, S.H. Almeida, R.M.B. Silveira and R.M.C. Santana: Int. Biodeterior. Biodegradation **109** (2016) 11–22.
16) A. Nourbakhsh and A. Ashori: Compos. Mater. **43** (2009) 877–883.
17) S.K. Chattopadhyay, R.K. Khandal, R. Uppaluri and A.K. Ghoshal: J. Appl. Polym. Sci. **119** (2011) 1619–1626.
18) O.T. Ikkala, R.M. Holsti-Miettinen and J. Seppälä: J. Appl. Polym. Sci. **49** (1993) 1165–1174.
19) H.S. Moon, B.-K. Ryoo and J.-K. Park: J. Polym. Sci., B, Polym. Phys. **32** (1994) 1427–1435.
20) G. Haddou, J. Dandurand, E. Dantras, D.H. Mai, H. Thai, V.G. Nguyen, H.T. Tran, P. Ponteins and C. Lacabanne: J. Therm. Anal. Calorim. **129** (2017) 1463–1469.
21) T. Wang, D. Liu and C. Xiong: J. Mater. Sci. **42** (2007) 3398–3407.
22) D.H. Mai, Q.T. Do, V.C. Do, H.T. Tran and V.G. Nguyen: Vietnam J. Sci. Technol. **56**(3B) (2018) 199–208.
23) N.M. Stark and L.M. Matuana: Polym. Degrad. Stabil. **92** (2007) 1883–1890.
24) S. Gogolewski: Colloid Polym. Sci. **257** (1979) 811–819.
25) G. Haddou, J. Dandurand, E. Dantras, D.H. Mai, H. Thai, V.G. Nguyen, H.T. Tran, P. Ponteins and C. Lacabanne: J. Appl. Polym. Sci. **136** (2019) 47623.
26) G. Haddou, J. Dandurand, E. Dantras, D.H. Mai, H. Thai, V.G. Nguyen, H.T. Tran, P. Ponteins and C. Lacabanne: J. Therm. Anal. Calorim. **124** (2016) 701–708.
27) D. Eloilson, M.C.P. Thieres, V.R.C. Eustáquio, R. Wanderson, L.S. Geovane and C.L.G. Regina: Polimeros **23** (2013) 37–41.
28) B. Marek and E. Lerch: J. Soc. Dyers Colour. **81** (1965) 481–487.